



Modelling nitrogen assimilation of *Escherichia coli* at low ammonium concentration

Hongwu Ma^a, Fred C. Boogerd^b, Igor Goryanin^{a,*}

^a Computational Systems Biology, School of Informatics, the University of Edinburgh, Informatics Forum, 10 Crichton Street, Edinburgh, EH8 9AB, UK

^b Department of Molecular Cell Physiology, Faculty of Earth and Life Sciences, Vrije Universiteit, Amsterdam, The Netherlands

ARTICLE INFO

Article history:

Received 7 May 2009

Received in revised form 28 August 2009

Accepted 4 September 2009

Keywords:

E. coli

Ammonium assimilation

Modelling

AmtB

Ammonium transport

ABSTRACT

Modelling is an important methodology in systems biology research. In this paper, we presented a kinetic model for the complex ammonium assimilation regulation system of *Escherichia coli*. Based on a previously published model, the new model included AmtB mediated ammonium transport and AmtB regulation by GlnK. Protein concentrations and several parameter values were determined or refined based on new experimental data. Steady state analysis of the model showed that the expression of AmtB increased the ammonium assimilation rate 4–5-fold at external ammonium concentrations as low as 5 μM . Model analysis also suggested that AmtB and GS levels were coupled to maximize the assimilation flux and to avoid a possible negative ammonia diffusion flux. In addition, model simulation of the short term dynamic response to increased external ammonium concentrations implied that the maximal rate for GlnB/GlnK uridylylation/deuridylylation might be higher for a quick response to environmental changes.

© 2009 Elsevier B.V. All rights reserved.

1. Introduction

The transport of ammonia/ammonium (referred to as Am in the paper) is fundamental to nitrogen metabolism (Reitzer, 2003). *Escherichia coli* has the ability to grow at Am concentrations even less than 5 μM by expressing an Am transport protein AmtB (Javelle et al., 2007). The *E. coli* AmtB protein is a member of the ubiquitous Amt family of ammonium transporters. Its structure has been determined at high resolution (1.35 Å) (Khademi et al., 2004). The revealed protein structure and related molecular dynamics model analysis suggested that AmtB functions as a channel protein (Fong et al., 2007; Javelle et al., 2008; Khademi et al., 2004; Lin et al., 2006; Luzhkov et al., 2006; Yang et al., 2007; Zheng et al., 2004). AmtB binds NH_4^+ at the entrance gate of the channel, deprotonates it and conducts NH_3 into the cytoplasm. Whether the uptake process is entirely based on facilitated diffusion or perhaps directly or indirectly coupled to the proton-motive force is a matter of debate. The Am transport process mediated by AmtB is regulated at different levels. In *E. coli*, the gene encoding AmtB forms an operon with *glnK*

that is transcriptionally regulated by the NtrBC two component system. Both AmtB and GlnK are only expressed at low Am availability. When the external Am concentration is higher than 50 μM , free diffusion of NH_3 through the cell membrane can provide enough nitrogen for cell growth and AmtB is not needed (Javelle et al., 2004). GlnK is a regulatory protein which shows high sequence similarity to an important nitrogen signalling protein: PII (encoded by *glnB*, referred to as GlnB in the following as in previous studies PII often represented a mixture of GlnB and GlnK). Interestingly, the function of GlnK is to bind with AmtB to block Am transport (Durand and Merrick, 2006; Gruswitz et al., 2007; Javelle and Merrick, 2005). However, at low Am concentration, GlnK is uridylylated by the same UTase/UR that uridylylates GlnB. The uridylylated GlnK (three UMP groups can be added to GlnK forming GlnKUMP1, GlnKUMP2 and GlnKUMP3) is not active in binding AmtB. Increased Am concentration (>50 μM) can shift the balance toward deuridylylation, activating GlnK to block AmtB mediated transport. Therefore GlnK functions as a brake to turn off Am transport quickly when it is not required.

Kinetic modelling is an important approach in systems biology which can offer in-depth quantitative understanding of complex biological systems and generate valuable predictions. Kinetic models for various metabolic pathways and regulatory circuits have been developed. However, only a few modelling analyses have been reported for the Am assimilation pathways. A notable work was from Bruggeman et al. (2005) who developed an integrated model (referred to as B-model) for Am assimilation in *E. coli* including multifarious regulation such as the adenylation of GS and uridy-

Abbreviations: Am, $\text{NH}_3 + \text{NH}_4^+$; AKG, alpha-ketoglutarate; GLU, glutamate; GLN, glutamine; GS, glutamine synthetase; GDH, glutamate dehydrogenase; GOGAT, glutamate synthase; UT, uridylyl transfer; UR, uridylyl removal; deAD, deadenylylation; AD, adenylylation; J_N , total N assimilation rate; J_D , flux through diffusion; J_{AmtB} , flux through AmtB; J_{GS} , flux through GS; J_{GDH} , flux through GDH; DCW, dry cell weight; B-Model, model by Bruggeman et al.

* Corresponding author. Fax: +44 131 650 6899.

E-mail address: goryanin@inf.ed.ac.uk (I. Goryanin).

ylation of GlnB. This model was used successfully to simulate the steady state and transient response behaviour of *E. coli* at different (internal) Am concentrations. However, an important process missing in the model is the Am transport process. Neither passive NH_3 diffusion nor AmtB mediated Am transport were included in the model. Therefore it cannot be used to study the Am assimilation behaviour at low external Am concentration and how the cells respond to external Am changes. Based on this work, we have developed a new model which includes the transport reactions and the related regulatory interactions. Most parameters in the model, including concentrations of metabolites and proteins, are based on experimental data obtained from literature. We used this new model to simulate the cellular behaviour at a wide range of external Am concentrations.

2. Model construction

2.1. Reactions in the model

At low Am, the ammonium assimilation process consists of the following steps as shown in Fig. 1: Am transport by AmtB and diffusion, intracellular NH_4^+ uptake by GS/GOGAT/GDH and exchange reactions for GLU, GLN (for protein synthesis and amino group transfer). The reaction equations for the various processes are shown in Appendix A.

The AmtB mediated transport reactions are based on what is known about the transport mechanism. The mechanism by which AmtB conducts Am into the cytoplasm has been extensively studied. Although there are still controversial aspects on details of the transport process, a widely recognized mechanistic view is that NH_4^+ binds to AmtB at the entrance gate and is deprotonated, while NH_3 is transported via a channel into the cytoplasm and reprotonated (Bostick and Brooks, 2007; Fong et al., 2007; Javelle et al., 2008; Khademi et al., 2004; Lin et al., 2006).

The following four reactions were used for the AmtB mediated Am transport process (the subscripts “in” and “ex” denote intracellular and extracellular, respectively):

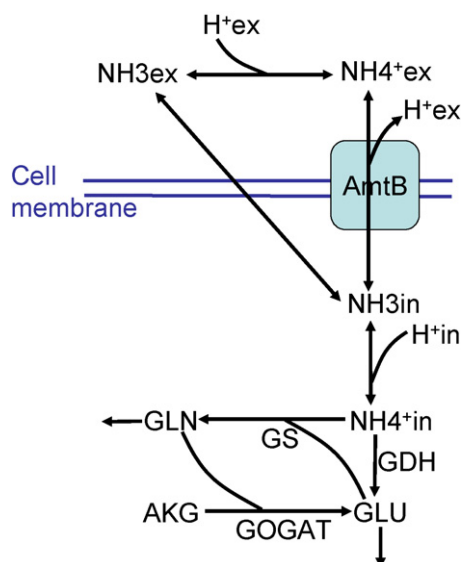
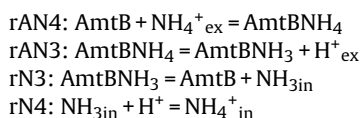


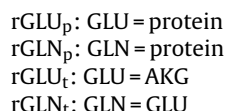
Fig. 1. Ammonium assimilation network at low ammonium concentration.

The first reaction (rAN4) is for the exterior NH_4^+ binding at the periplasmic gate of AmtB (site Am1) (Bostick and Brooks, 2007; Khademi et al., 2004). At this site, the pK_a of NH_4^+ was shifted from 9.25 to below 6, thereby shifting the equilibrium of the second reaction (rAN3) toward the production of AmtBNH₃. The generated proton is released into the periplasm. NH_3 then passes through several binding sites in the channel (sites Am2, Am3 and Am4) and is finally released at the cytoplasmic gate (rN3). In the cytoplasm, virtually all NH_3 is converted to NH_4^+ (rN4), because intracellular pH (7.5) is far below the pK_a of NH_4^+ .

In addition to the AmtB mediated Am transport process, NH_3 can also be transported through the membrane by passive diffusion. As calculated by Bruggeman et al. (2005), just a 29 nM NH_3 gradient over the membrane is already enough to get an Am assimilation flux sufficient for a moderate growth rate. Therefore we need to include the passive NH_3 diffusion process in our model, even at low Am concentration.

AmtB activity can be blocked by binding with GlnK when the environmental Am concentration is increased. GlnK is uridylylated by the same UTase/UR that uridylylates GlnB. Reaction equations similar to the GlnB uridylylation/deuridylylation reactions in the B-model were used to represent the GlnK modification processes in our model (Appendix A). However, we made a distinction between the regulatory function of GlnB and GlnK: only GlnB was assumed to be involved in the regulation of GS adenylylation, whereas only GlnK was used for blocking AmtB. This is based on the experimental evidence that even though GlnB can also bind with AmtB in vitro, it does not affect the AmtB activity for Am transport (Coutts et al., 2002). Considering that at low Am concentration there is more GlnK than GlnB and the most GlnB is uridylylated, we chose to ignore the GlnB–AmtB binding process. It has also been reported that GlnK is 40 times less active than GlnB in stimulating adenylylation of GS (Reitzer, 2003). Therefore we also ignore the GlnK regulation of GS in our model.

Exchange reactions for GLU and GLN were introduced in the model, while the AKG concentration was fixed as in the B-model. However, differing from the B-model, we introduced two different exchange reactions for each of the two metabolites as shown below:



The subscript “p” denotes that the exchange reaction represents all the reactions in which the corresponding amino acid (GLU or GLN) and its derived amino acids are used in protein synthesis. The subscript “t” denotes that the exchange reaction represents all the reactions in which the corresponding amino acid is used for amino group transfer. We distinguish the two processes because the carbon backbone of GLU and GLN can be reused in the amino transfer reactions but not in the protein synthesis reactions.

Other reactions in the model such as the metabolic reactions by GS, GOGAT and GDH, GlnB uridylylation/deuridylylation, GS adenylylation/deadenylylation were introduced directly from the B-model. The full list of reactions in the model can be seen in Appendix A.

2.2. Metabolite and protein concentrations

2.2.1. Concentrations of metabolites

As the first step, we ignore the transport through the outer membrane of the cell and assume that the Am concentrations in the periplasm and the extracellular medium are equal.

The external Am concentration is set to fixed values. Then from the pK_a value of NH_4^+ (9.25) the external NH_4^+ and NH_3 concen-

Table 1
Fixed metabolite and protein concentrations used in the model.

Proteins or metabolites	Concentration (mM)
ATP	4
ADP	1.4
NADP	0.05
NADPH	0.15
AKG	1
AmtB (total)	0.0005
GlnK (total)	0.002
GlnB (total)	0.00065
GS (total)	0.012

tration can be calculated as:

$$\text{NH}_{4\text{ex}}^+ = \frac{\text{Am} \times \text{H}_{\text{ex}}^+}{\text{Ka} + \text{H}_{\text{ex}}^+} \quad (1)$$

$$\text{NH}_{3\text{ex}} = \frac{\text{Am} \times \text{Ka}}{\text{Ka} + \text{H}_{\text{ex}}^+} \quad (2)$$

The external pH is set to 7.0 and the cytoplasmic pH is taken to be 7.5 based on previous observations. Almost all Am exists as NH_4^+ at these pH values.

The intracellular concentrations for ATP, ADP, NADP, NADPH and AKG are assumed to be constant (values are shown in Table 1 and are mainly based on the B-model) to avoid introducing exchange fluxes for these metabolites. The physiological concentration range of AKG is 0.1–1 mM (Bruggeman et al., 2005). Under N starvation condition, AKG concentration is increased, while GLU and GLN concentrations are decreased. Therefore we set AKG concentration at 1 mM in our model.

For the compartmentalised model, we need to determine the volume ratio of external medium over internal cytoplasm. Assuming that an *E. coli* cell suspension of OD600 = 1 contains 0.45 mg dry cell weight/ml medium (Fong et al., 2007) and that 1 mg dry weight is equivalent to 2 μl of internal cell volume (Ikeda et al., 1996), the volume of the medium is 900 times the volume of the cells. It should be noted that this value is of course not constant but depends on the cell density. For convenience, we take the volume ratio to be 1000 (medium volume is 1000 ml, cell volume is 1 ml).

2.2.2. Protein concentrations

Javelle et al. (2004) reported that at very low Am concentration, GlnK can be 500 times more than GlnB which is constitutively expressed. However, van Heeswijk et al. (2009) reported that the GlnK/GlnB ratio was less than 2 in media without ammonium. The measured GlnB and GlnK levels were 87 ng/mg protein and 143 ng/mg protein, respectively. Assuming that 55% of the dry cell weight is protein (Nielsen et al., 2003) and that 1 mg dry weight equals to 2 μl cell volume (Ikeda et al., 1996), the levels are equal to concentrations of 0.65 μM (GlnB) and 1.1 μM (GlnK). The low GlnK/GlnB ratio may be partly due to the high glutamine concentration (14 mM) in their culture media. The total GlnK plus GlnB concentration (1.8 μM) is also somewhat less than reported previously (3 μM) by the same author (Heeswijk, 1998). Considering these different results, we assumed a GlnB concentration of 0.65 μM and a GlnK concentration of 2.0 μM , mainly based on the new result by van Heeswijk et al. (2009). A similar GlnB concentration was found in a recent proteomics study with *E. coli* (Ishihama et al., 2008). They reported that the number of GlnB monomers per cell was 600. Assuming that the *E. coli* cell volume is $0.79 \times 10^{-18} \text{ m}^3$ (Bruggeman et al., 2005), the GlnB trimer concentration is calculated to be 0.4 μM .

No direct measurement of the AmtB concentration was found in the literature. However, it is possible to estimate the AmtB concentration indirectly as follows: Zheng et al. (2004) reported that AmtB

can move ammonia at a rate 10–10,000 molecules/s per channel depending on the Am concentration. Javelle et al. (2007) reported a single channel conductance rate of about 3×10^4 molecules of NH_3/s at an ammonium concentration of 5 mM. Based on these results, we calculated that 40–0.014 μM AmtB trimer is required to reach a 25 mM/min N assimilation flux at a growth rate of 0.3 h^{-1} (Bruggeman et al., 2005). Considering that the growth rate will be lower at low Am concentration, the required AmtB concentration should then be less than roughly 20 μM .

AmtB and GlnK are in the same operon and the main function of GlnK is to block AmtB mediated transport when external Am is increased. Therefore we can use the measured GlnK concentration to further refine the possible AmtB concentration range. Normally the first gene in an operon has a higher expression level than other genes in the same operon. Moreover, the GlnK concentration is expected to be higher than the AmtB concentration to allow for an efficient blocking of AmtB upon a sudden increase in ammonium availability. Therefore we initially set the AmtB trimer concentration at 0.5 μM , one fourth of the GlnK concentration. This is equal to around 225 channels per cell, which is higher than the 56 channels per cell calculated by Javelle et al. (2007). The main reason for the difference is the very high conductive rate at high Am concentration (5 mM) used in their calculation.

The concentration of GS used in the B-model was 14 μM (Bruggeman et al., 2005). In the recent study by van Heeswijk et al. (2009), GS concentration was measured to be 24–30 $\mu\text{g}/\text{mg}$ protein, which represents 11–13 μM . We initially set the value at 12 μM , but it was changed later as further discussed in Section 3.2.

2.3. Kinetic equations for the reactions

2.3.1. Kinetic equations for AmtB mediated transport

Reversible mass action kinetics was used for the AmtB mediated transport reactions (Appendix B). We assume that the two binding reactions (rAN4 , rN3) are fast reactions. The parameter values were chosen such as to make the rate of the forward reaction similar to the rate of the backward reaction. The conversion of AmtBNH_4 to AmtBNH_3 (rAN3) was assumed to be the rate limiting step. As described in Section 2.1, the pK_a of NH_4^+ was below 6 in the channel. Therefore we set the dissociation constant at 10^{-6} . Because pK_a is lower than the pH value, there should be more AmtBNH_3 than AmtBNH_4 at steady state. This is in contrast with the fact that the majority of Am exists as NH_4^+ in the medium and inside the cell. The value of k_{AmtB} was initially set at 2000, resulting in a forward reaction rate of 0.2 mM/s assuming that AmtBNH_4 is one fifth of the total AmtB. This parameter will be further investigated in the model analysis section.

In the cytoplasm, NH_3 is protonated again because the intracellular pH is about 7.5. This is a fast reaction, the parameter values of which are determined based on the pK_a value of 9.25.

2.3.2. Kinetic equations for the metabolic and regulatory reactions

The kinetic equations for most of the metabolic and regulatory reactions are based on the B-model. However, the kinetic equation for GS in the B-model is not suitable, because it required either that the NH_4^+ concentration was higher than 7.5 μM (at the set ATP and ADP concentrations) or that the GLU/GLN ratio was increased to make the GS reaction run in the forward direction. The kinetic equation for GS is therefore based on the equation used in the model developed by Demin et al. (unpublished result, Appendix B). For GOGAT, the kinetic equation in the B-model contains a variable MET_{GLU} that is not in our model, because we represent the exchange reactions in a different way. It should be mentioned that, although we use kinetic equations from previous studies, we had to change some parameter values to have reasonable simulation results. We

will have more discussion on parameter fitting in Section 3. A list of parameter values in the model can be found in Appendix B.

The kinetic equations for GlnK uridylylation/deuridylylation are the same as those for GlnB modification. However we changed the K_{GLN} parameter for GlnB of 0.07 to 0.04 mM for GlnK so that GlnK responds to lower GLN concentrations than GlnB.

2.3.3. Determination of NH_3 diffusion rate

Based on Fick's diffusion law, we have the following rate equation for free diffusion of NH_3 across the cell membrane:

$$J = \frac{P \times A_{cell} \times \Delta NH_3}{V_{cell}} = k_{NH_3} \times (NH_{3ex} - NH_{3in}) \quad (3)$$

Very different values for the NH_3 permeability coefficient P were reported in previous studies. In the B-model, P was set at 2 mm/s, a value which was based on measurements with liposomes by Mathai et al. (2001). The values measured for whole cells are much lower though (Kleiner, 1985; Winkler, 2006). For example, Kleiner (1985) obtained a value of 0.02 mm/s for *Klebsiella pneumoniae*. However, such a low permeability coefficient may lead to very low N assimilation flux at low Am concentration. Based on Eq. (2), the NH_3 concentration is only 0.28 μM at pH 7.0 when the Am concentration is 50 μM (a concentration that allows diffusion alone to maintain growth). Therefore, based on the *E. coli* cell surface area and volume values from the B-model (5.6×10^{-6} and 0.79×10^{-9} mm³, respectively) (Bruggeman et al., 2005), the maximal N assimilation flux (when $NH_{3in} = 0$) is only 0.04 mM/s at $P = 0.02$ mm/s. This is only about 10% of the assimilation flux required for a growth rate at 0.3 h⁻¹. The low P value obtained by Kleiner (1985) may be related to the high Am concentration used in his study (20 mM Am, 11.2 μM extracellular NH_3 concentration). Considering these facts, we set the P value at 0.15 mm/s in our model. The value of k_{NH_3} was then calculated to be 1050 s⁻¹.

2.3.4. Kinetics for the exchange reactions

As described in Section 2.1, four exchange reactions were introduced for GLU and GLN to represent the corresponding amino transfer reactions and protein synthesis reactions. An exchange reaction is a sum of many reactions and therefore it is impossible to determine the kinetics based on reaction mechanisms. For simplicity, Michaelis–Menten kinetics was used for all four exchange reactions. The K_m value is based on the physiological concentration ranges of GLN (0.1–1 mM) and GLU (1–10 mM). The V_m value is based on the total N flux and ratios from the review paper by Reitzer (2003). Based on the chemical composition of an *E. coli* cell, Reitzer calculated that 0.25 mmol GLU/gDCW and 0.25 mmol GLN/gDCW are used for protein synthesis. In addition, the carbon backbone of 0.56 mmol GLU/gDCW is also used in synthesis of other amino acids such as arginine and proline. Thus the total biosynthetic requirement for GLU is 0.81 mmol/gDCW. The amount of GLU used for amino group transfer is calculated to be 7.1 mmol/gDCW and that of GLN 2.1 mmol/gDCW. Based on these data, we set the V_m values for the four exchange reactions (Appendix B) such that the ratios between the V_m values are consistent with the different biosynthetic requirements of GLN and GLU.

3. Model analysis

3.1. Ammonium assimilation without AmtB, refining parameters

We need to first test the model without AmtB to make sure that at 0.05 mM Am the N flux required for growth can be maintained by diffusion alone. We did this by removing the AmtB transport reactions from the model. Then all the intracellular Am are transported by the diffusion process. The steady state was calculated using Copasi (Hoops et al., 2006). We noticed that in the B-model the

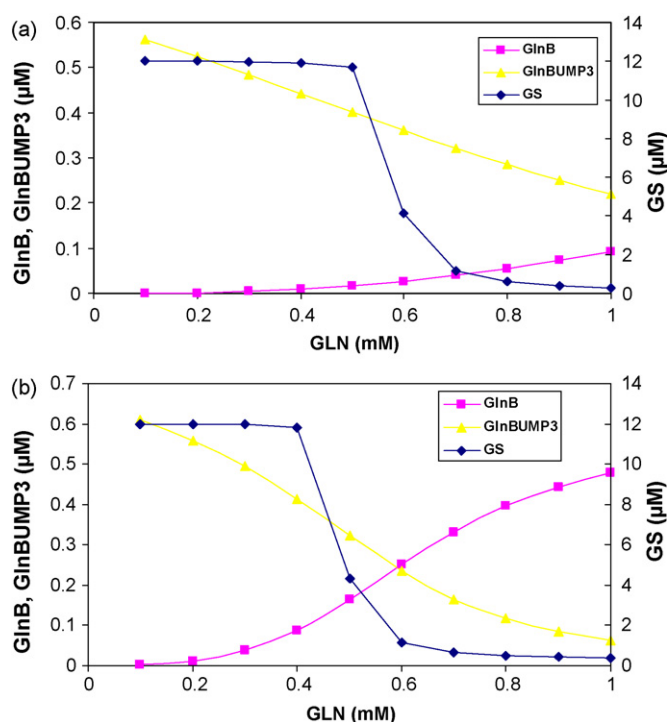


Fig. 2. Effect of GLN concentration on GlnB and GS activity calculated from the model. (a) Using parameter values from the B-model; (b) using revised parameters: V_{UR} for rUR1 was changed from 0.0033 to 0.033 mM/min, V_{AD} for rAD was changed from 0.5 to 0.03 mM/min.

steady state GLN concentration is high (0.9 mM) even at 0.05 mM intracellular Am concentration (Table 2 in their paper) (Bruggeman et al., 2005). More surprisingly, only about 15% of GlnB is in the unuridylylated state even when GLN is at 1 mM (Fig. 2a in their paper). According to previous research results, high GLN is a signal of high nitrogen availability and thus GlnB should be in the active form to turn down ammonium assimilation. To address this problem, we increased V_{UR} in the kinetic equation of the deuridylylation reaction from 0.055 to 0.55 $\mu M/s$ to shift the balance toward GlnB. As shown in Fig. 2b, the result is much better. We also changed V_{DEAD} in the GS adenylation reaction from 8 to 50 $\mu M/s$ so that GS activity (represented as free GS concentration) mainly changes in the GLN concentration range from 0.4 to 0.6 mM, as in the B-model.

We used the refined parameters to calculate the steady state at 0.05 mM extracellular Am concentration. Although a reasonable N flux (0.23 mM/s) was obtained, the steady state GLN concentration was unreasonably low (0.045 mM), whereas the steady state GLU concentration would be very high (112 mM). We analyzed the model and found that the high maximal rate of GOGAT was the main cause for this strange behaviour. We changed V_{GOG} from 1.4 to 0.3 mM/s and calculated the steady states for a wide range of external NH_4^+ concentrations (from 0.05 to 0.5 mM). Table 2 shows that both GLN and GLU are in a physiologically reasonable range. The N flux through GDH (J_{GDH}) is increased 20 times which is consistent with the results from the B-model. However, despite the fact that active GS is decreased nearly 20 times, the N assimilation flux through GS (J_{GS}) does not change much mainly due to the greatly increased intracellular NH_4^+ concentration. This may imply that protein level regulation of GS activity (by GlnB) alone is not enough for the proper control of the biosystem. Gene level regulation of GS through the NtrBC system may be needed to reduce the flux through GS to a minimal level. The current model will focus on the short term protein regulation behaviour of the ammonium assimilation system. We can extend it to include

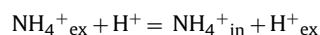
Table 2
Steady state fluxes and concentrations of the diffusion model at different Am concentrations.

Am (mM)	J_N (mM/s)	J_{GS} (mM/s)	J_{GDH} (mM/s)	GLN (mM)	GLU (mM)	NH _{4in} (mM)	GS (μ M)	GlnB (μ M)
0.05	0.20	0.19	0.01	0.23	1.5	0.005	12	0.02
0.1	0.28	0.26	0.03	0.49	2.7	0.015	5.2	0.16
0.2	0.34	0.26	0.08	0.54	4.5	0.043	2.1	0.20
0.3	0.38	0.25	0.12	0.58	7.0	0.070	1.3	0.24
0.4	0.41	0.25	0.16	0.63	10.6	0.099	0.9	0.28
0.5	0.43	0.24	0.18	0.69	14.9	0.127	0.7	0.32

gene regulation when more related experimental data will be available.

3.2. Function of AmtB/GS at low Am concentration

Without AmtB, the simulated N assimilation flux (J_N) drops below 0.1 mM/s when the external Am concentration is less than 20 μ M. At 5 μ M Am, J_N is just 0.02 mM/s and the concentrations of GLN and GLU are very low (at 0.01 and 0.1 mM, respectively). This indicates the necessity of AmtB mediated transport to maintain *E. coli* growth at such a low ammonium concentration. To test how AmtB mediated transport affects J_N and the intracellular metabolite concentrations, we calculated the steady states for different k_{AmtB} values at 5 μ M Am. As shown in Table 3, J_N was increased 3–6 times with an increased AmtB transport rate (J_{AmtB}). The intracellular concentrations of GLU and GLN are also increased to levels close to the experimentally measured physiological range. However, a surprising simulation result is the negative ammonia diffusion flux (J_D) caused by the higher intracellular NH₃ concentration. Considering that AmtB is a channel protein and there is no energy consumption during the transport process, it is quite arguable how a real cell could maintain a higher intracellular NH₃ concentration. However, a recent experimental study on *E. coli* AmtB transport by Fong et al. (2007) has shown that the intracellular methylammonium concentration could be 100 times higher than the extracellular concentration. Although membrane diffusion of ammonia may be different from that of methylammonia, this result suggests that *E. coli* could possibly maintain a negative diffusion flux by coupling with other energy consuming processes. A fact often overlooked in previous studies is that the proton is not balanced in the AmtB mediated transport process. One proton is released to the extracellular environment while a proton is consumed for the protonization of NH₃ inside the cell. The overall reaction equation is

**Table 3**
Effect of k_{AmtB} on the steady state fluxes and concentrations at low Am concentration (5 μ M). GS at 12 μ M.

k_{AmtB} (1/s)	J_N (mM/s)	J_D (mM/s)	J_{AmtB} (mM/s)	AmtBGlnK (μ M)	GLN (mM)	GLU (mM)	NH _{3in} (nM)	NH _{4in} (μ M)
0	0.020	0.020	0	0	0.010	0.10	8.8	0.47
1000	0.062	0.001	0.061	0.008	0.037	0.33	27.0	1.44
2000	0.082	-0.008	0.090	0.020	0.053	0.46	35.6	1.90
3000	0.095	-0.014	0.109	0.032	0.065	0.54	41.1	2.19
4000	0.105	-0.018	0.123	0.045	0.074	0.61	45.1	2.41
5000	0.112	-0.021	0.133	0.057	0.081	0.66	48.2	2.57

Table 4
Effect of k_{AmtB} on the steady state fluxes and concentrations at low Am concentration (5 μ M). GS at 24 μ M.

k_{AmtB} (1/s)	J_N (mM/s)	J_D (mM/s)	J_{AmtB} (mM/s)	AmtBGlnK (μ M)	GLN (mM)	GLU (mM)	NH _{3in} (nM)	NH _{4in} (μ M)
0	0.024	0.024	0	0	0.013	0.12	5	0.27
1000	0.087	0.010	0.077	0.037	0.059	0.48	18	0.96
2000	0.115	0.005	0.110	0.095	0.087	0.67	23.6	1.26
3000	0.130	0.001	0.129	0.145	0.106	0.78	26.7	1.43
4000	0.140	-0.001	0.141	0.184	0.120	0.86	28.8	1.53
5000	0.148	-0.002	0.150	0.213	0.130	0.92	30.2	1.61

The intracellular pH is about 7.5 in *E. coli*. This represents a free hydrogen ion concentration of only 30 nM. Therefore even if the N assimilation flux is just say 0.2 mM/s, the intracellular pH might be quickly changed if there are no other reactions to balance the consumed hydrogen ions. In non-cellular AmtB containing proteoliposomes pH changed greatly in less than 0.1 s (Khademi et al., 2004). Therefore it seems likely that to keep the cytoplasmic pH constant certain other energy consuming, proton-producing reactions need to be coupled with AmtB mediated transport. Further experimental studies are required to verify this hypothesis.

Besides the up-regulation of AmtB, *E. coli* cells may also use other strategies to increase J_N at low Am concentration. Increasing the amount of GS through gene regulation is an obvious scenario. To test it, we increased the GS concentration from 12 to 24 μ M in the model and calculated steady states at different k_{AmtB} values as shown in Table 4. It can be seen that J_N is further increased (20–70%) by doubling GS. Furthermore, negative diffusion flux is avoided at low k_{AmtB} values. Considering that the expression levels of both GS and AmtB are regulated by the NtrBC two component system, the amounts of both GS and AmtB likely increase when the extracellular Am concentration changes from 50 to 5 μ M. Experimental measurements also suggested that GS and AmtB are coupled at the metabolic level to maintain the N assimilation flux at low Am concentration (Javelle et al., 2005). Another interesting finding from Table 5 is that at high k_{AmtB} values, a proportion of AmtB (nearly 10% at $k_{AmtB} = 5000 \text{ s}^{-1}$) is deactivated by binding with GlnK. In addition, the effect of k_{AmtB} on J_N at high k_{AmtB} is small. Therefore we decided to choose a k_{AmtB} value of 2000 s^{-1} for further model analysis. At this parameter value, J_N is 0.115 mM/s, which seems reasonable enough considering that at low Am concentration the growth rate is low. Note that the NH₃ diffusion flux contributes less than 5% to the N assimilation rate. For the metabolic reactions, GS is the major reaction for assimilation and GDH contributes only about 2% (data not shown).

Table 5
Steady state fluxes calculated from the model at different Am concentrations.

Am (μM)	J_N (mM/s)	J_D (mM/s)	J_{AmtB} (mM/s)	J_{GS} (mM/s)	J_{GDH} (mM/s)
5	0.115	0.005	0.110	0.112	0.002
10	0.153	0.026	0.127	0.150	0.003
20	0.188	0.077	0.111	0.185	0.004
50	0.260	0.223	0.037	0.254	0.006
100	0.292	0.239	0.053	0.257	0.035
200	0.343	0.268	0.075	0.257	0.086
500	0.431	0.323	0.108	0.246	0.185
1000	0.480	0.350	0.130	0.255	0.224

Table 6
Steady state concentrations at different Am concentrations.

Am (μM)	AmtB (μM)	AmtBGlnK (μM)	AmtBNH ₄ (μM)	GlnK (μM)	GS (μM)	GlnB (μM)	GLN (mM)	GLU (mM)
5	0.150	0.095	0.073	0.006	24.0	0.001	0.087	0.67
10	0.078	0.217	0.076	0.028	24.0	0.004	0.138	0.96
20	0.032	0.339	0.062	0.106	24.0	0.012	0.207	1.27
50	0.004	0.460	0.020	1.122	19.1	0.131	0.472	2.10
100	0.003	0.407	0.032	1.233	4.6	0.158	0.507	2.84
200	0.002	0.338	0.049	1.361	2.0	0.197	0.557	4.78
500	0.001	0.235	0.073	1.579	0.7	0.322	0.729	16.03
1000	0.001	0.162	0.090	1.776	0.3	0.525	1.555	47.40

3.3. Steady states at different Am concentrations

We first used the model to investigate how the extracellular Am concentration affects the steady state fluxes and concentrations. The results are shown in Tables 5 and 6, respectively. Even without gene regulation, the model generates reasonable results in

the range of 5–1000 μM Am. J_N increases only four times when the extracellular Am concentration is increased by a factor of 200. The diffusion flux steadily increases with increasing Am concentration and the flux through GDH increases about 70 times. However, the flux through GS also increases despite the greatly reduced active GS concentration. This is mainly because the intracellular ammonium

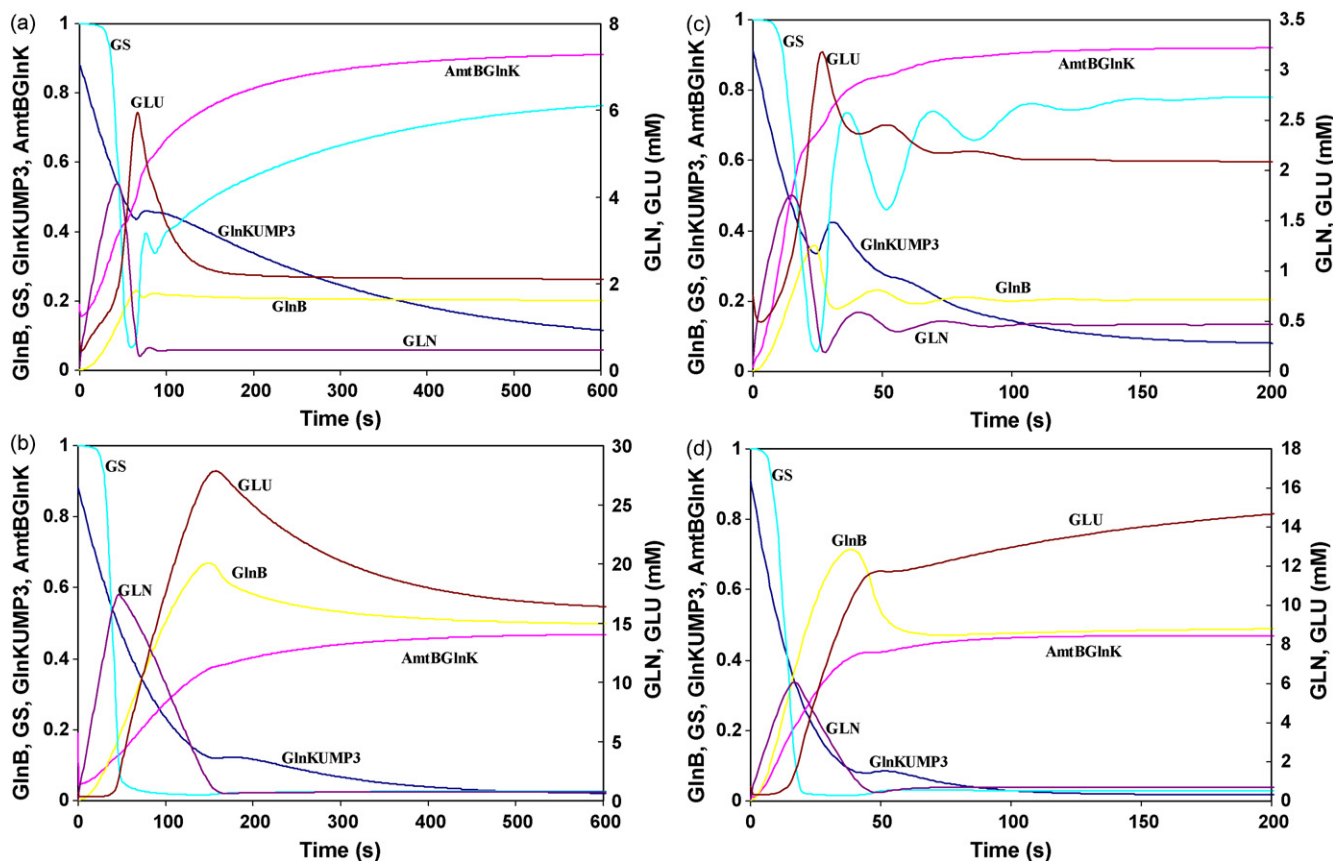


Fig. 3. Model simulation of transient responses to sudden increases of Am concentration from 5 to 50 μM (a and c) or 500 μM (b and d). Protein concentrations are normalized by dividing by the total concentrations of AmtB, GlnK, GlnB and GS. (a and b) Using parameter values from the B-model for the uridylylation and deuridylylation reactions except that V_{UR} for rUR1 and rGUR1 is increased 10-fold. (c and d) using revised parameter values, all the maximal rates for GlnB/GlnK modification were increased five times.

concentrations are also greatly increased (37 times when extracellular Am from 50 to 500 μM) but still just 0.13 mM, close to the K_{m,NH_4} value of 0.1 mM (Appendix B). This implies that GS may have a lower K_m value for ammonium. More interestingly, the blocked AmtB (AmtBGlnK) reaches the highest level at about 50 μM and decreases again when the Am concentration is further increased in spite of the fact that most GlnK is deuridylylated at high Am concentrations. An explanation for this paradoxical phenomenon is that at high Am concentrations, the high NH_4 and NH_3 concentrations push the balance in the binding reactions (rAN4 and rN3) toward the production of AmtBNH4 and AmtBNH3, and thereby less free AmtB is available for the formation of AmtBGlnK. In real cells, increasing Am concentrations will also trigger the gene regulation process to reduce the amount of AmtB as well as GS in addition of the protein level regulation. It has been reported that the total GS concentration is only about 1.6 μM at high Am concentration (van Heeswijk et al., 2009), 15-fold lower than that used in the model (24 μM). Therefore it is important to include gene regulation processes in the model for a complete description of the regulation behaviour at a wide range of Am concentrations. The current model is more suitable to simulate the short term behaviour where regulation is mainly at the protein level.

3.4. Transient response to an Am pulse

To simulate how *E. coli* cells respond to a sudden increase of the extracellular Am concentration, we used the steady state at 5 μM Am as the initial condition for the simulation and then changed the Am concentration to 50 or 500 μM at time zero to calculate the concentration changes over time using Copasi (Hoops et al., 2006). The results are shown in Fig. 3a and b. GLN and GLU concentrations are increased quickly in the first minute, because most AmtB and GS are still active. GLN concentration peaks at 4 mM within a minute at 50 μM Am (Fig. 3a). This result is in agreement with the experimental results reported by Javelle et al. (2004). They reported that GLN concentration increased 30-fold in just 30 s when the Am concentration was increased to 50 μM . However, a much higher peak concentration of GLN (16 mM) is reached at 500 μM Am (Fig. 3b). This implies that in that case an even faster shut off of AmtB and GS would be required. GlnKUMP3 deuridylylation takes about 4–10 min depending on the Am concentration. However, only about 40% AmtB is blocked (represented as AmtBGlnK in Fig. 3b) is low at 500 μM Am. This result is also reflected by the low steady state AmtBGlnK concentrations in Table 6. As explained in Section 3.3, this abnormal phenomenon is mainly because of the formation of AmtBNH4 and AmtBNH3. In contrast to the slow response of GlnK and the ineffective shutdown of AmtB, GS is shut off quickly (more than 90% deactivated in 60 s, Fig. 3a). In spite of the fact that only about 20% of GlnB is deuridylylated upon the 50 μM Am upshift in Am. The main factor affecting the adenylation of GS at this short time scale is GLN. GlnB as only 20% of GlnB is activated in the first minute. The kinetic equation for GS adenylation in Appendix B does show that the adenylation rate increases with GLN concentration. This also explains why active GS is increased again after 1 min when the GLN concentration drops to a low level. This quick response to metabolites rather than to proteins may be important for *E. coli* to survive in a rapidly changing environment. Otherwise the GLN concentration would increase in a short time to levels that might be toxic to the cell. In contrast to GS's quick response to metabolites, the response of the regulatory proteins is relatively slow (GlnKUMP3 and GlnB in Fig. 3a and b). To obtain a quick response, we increased the maximal rates of the GlnB and GlnK modification reactions to five times their original values in the B-model (this does not affect the steady state as all rates are increased). The simulated dynamic behaviour is shown in Fig. 3c and d. For both upshifts, GlnK and GlnB reach a level near

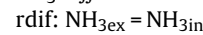
their steady states in about one minute (GlnKUMP3 deuridylylation takes a little bit longer at 50 μM Am upshift). The fast regulation even causes oscillation of GS, GLN, GLU and GlnB concentrations at the 50 μM Am upshift (Fig. 3d). The peak concentrations of GLN (2 mM in Fig. 3c and 6 mM in Fig. 3d) are also reduced by the fast protein level regulation. In addition, the period that the cells experience high GLN concentration is reduced from 45 (Fig. 3a, b) to 15 s (Fig. 3c and d). Based on these results, we suspect that *E. coli* may have a faster uridylylation/deuridylylation rate than that used in the B-model.

Acknowledgement

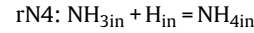
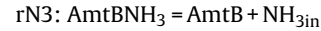
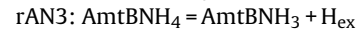
This work is supported by EC-MOAN, a research project supported by 6th European Framework Programme FP6-2005-NEST-PATH-COM.

Appendix A. List of reactions in the model.

NH₃ diffusion:



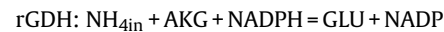
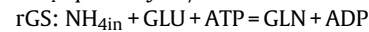
AmtB transport:



AmtB GlnK binding:



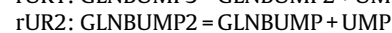
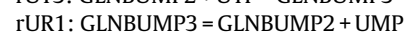
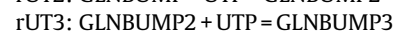
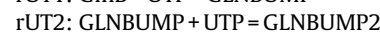
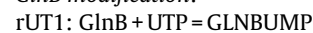
NH₄ uptake by GS/GOGAT and GDH:



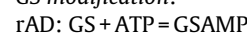
Exchange reactions for GLU, GLN:



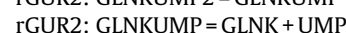
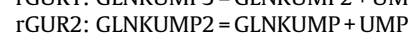
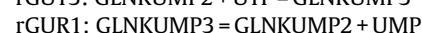
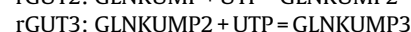
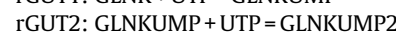
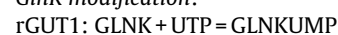
GlnB modification:



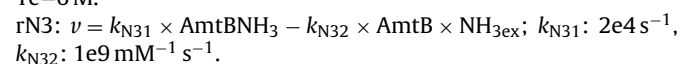
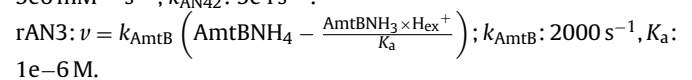
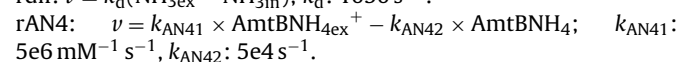
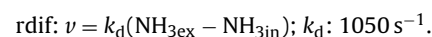
GS modification:



GlnK modification:



Appendix B. Kinetic equations and parameter values for the reactions in the model



$$rN4: v = k_{N41} \times H_{in}^+ \times NH_{3in} - k_{N42} \times NH_{4in}^+; k_{N41}: 1e12 \text{ mM}^{-1} \text{ s}^{-1}, k_{N42}: 5.62e5 \text{ s}^{-1}.$$

$$rAG: v = k_1 \times \text{AmtB} \times G \ln K - k_2 \times \text{AmtBG} \ln K; k_1: 1e10 \text{ mM}^{-1} \text{ s}^{-1}, k_2: 100 \text{ s}^{-1}.$$

$$rGS: v = \frac{k_{GS} \times GS}{(K_{m_ATP}/ATP) + (K_{m_GLU}/GLU) + (K_{m_NH_4}/NH_{4in}^+)}; k_{GS}: 400 \text{ s}^{-1}, K_{m_ATP}: 0.4 \text{ mM}, K_{m_GLU}: 3.9 \text{ mM}, K_{m_NH_4}: 0.1 \text{ mM}.$$

$$rGOG: v = \frac{V_{GOG} (GLN \times AKG \times NADPH / K_{GLN} \times K_{AKG} \times K_{NADPH})}{(1 + (GLN/K_{GLN}) + (GLU/K_{GLU})) (1 + (AKG/K_{AKG}) + (GLU/K_{GLU})) (1 + (NADP/K_{NADP}) + (NADPH/K_{NADPH}))}; V_{GOG}: 0.3 \text{ mM/s}, K_{GLN}: 0.175 \text{ mM}, K_{AKG}: 0.007 \text{ mM}, K_{NADPH}: 0.0015 \text{ mM}, K_{GLU}: 11 \text{ mM}, K_{NADP}: 0.0037 \text{ mM}.$$

$$rGLUp: v = \frac{v_{Up} \times GLU}{K_{Up} + GLU}; v_{Up}: 0.04 \text{ mM/s}, K_{Up}: 2.5 \text{ mM/s}.$$

$$rGLNp: v = \frac{v_{Np} \times GLN}{K_{Np} + GLN}; v_{Np}: 0.013 \text{ mM/s}, K_{Np}: 0.25 \text{ mM/s}.$$

$$rGLUt: v = \frac{v_{Ut} \times GLU}{K_{Ut} + GLU}; v_{Ut}: 0.35 \text{ mM/s}, K_{Ut}: 2.5 \text{ mM/s}.$$

$$rGLNt: v = \frac{v_{Nt} \times GLN}{K_{Nt} + GLN}; v_{Nt}: 0.1 \text{ mM/s}, K_{Nt}: 0.25 \text{ mM/s}.$$

$$rAG: v = k_1 \times \text{AmtB} \times G \ln K - k_2 v \text{AmtBG} \ln K; k_1: 300 \text{ mM}^{-1} \text{ s}^{-1}, k_2: 0.1 \text{ s}^{-1}.$$

rUT1 and rGUT1:

$$v = \frac{V_{UT} \times PII \times UTP}{(1 + (GLN/K_{GLN})) (K_{iPIIUMPj} \times K_{UTP} + K_{PIIUMPj} \times UTP + (K_{UTP} + UTP (1 + (PII/K_{PPi}))) (PII + PIIUMP + PIIUMP2) + K_{PIIUMPj} (K_{UTP}/K_{PIIUMPj} \cdot 1) (PIIUMP + PIIUMP2 + PIIUMP3))}$$

V.UT: 0.0014 mM/s, K_{GLN} : 0.07 mM (GlnB) and 0.04 mM (GlnK), $K_{iPIIUMPj}$: 0.0018 mM, K.UTP: 0.04 mM, $K_{PIIUMPj}$: 0.003 mM, K.PPi: 0.114 mM, $K_{PIIUMPj} \cdot 1$: 0.0035 mM.

$$rUT2 \text{ and } rGUT2: v = \frac{V_{UT} \times PIIUMP \times UTP}{(1 + (GLN/K_{GLN})) (K_{iPIIUMPj} \times K_{UTP} + (K_{UTP} + UTP (1 + (PII/K_{PPi}))) (PII + PIIUMP + PIIUMP2) + K_{PIIUMPj} (K_{UTP}/K_{PIIUMPj} \cdot 1) (PIIUMP + PIIUMP2 + PIIUMP3))}$$

V.UT: 0.0014 mM/s, K_{GLN} : 0.07 mM (GlnB) and 0.04 mM (GlnK), $K_{iPIIUMPj}$: 0.0018 mM, K.UTP: 0.04 mM, $K_{PIIUMPj}$: 0.003 mM, K.PPi: 0.114 mM, $K_{PIIUMPj} \cdot 1$: 0.0035 mM.

rUT3 and rGUT3:

$$v = \frac{V_{UT} \times PIIUMP2 \times UTP}{(1 + (GLN/K_{GLN})) (K_{iPIIUMPj} \times K_{UTP} + K_{PIIUMPj} \times UTP + (K_{UTP} + UTP (1 + (PII/K_{PPi}))) (PII + PIIUMP + PIIUMP2) + K_{PIIUMPj} (K_{UTP}/K_{PIIUMPj} \cdot 1) (PIIUMP + PIIUMP2 + PIIUMP3))}$$

V.UT: 0.0014 mM/s, K_{GLN} : 0.07 mM (GlnB) and 0.04 mM (GlnK), $K_{iPIIUMPj}$: 0.0018 mM, K.UTP: 0.04 mM, $K_{PIIUMPj}$: 0.003 mM, K.PPi: 0.114 mM, $K_{PIIUMPj} \cdot 1$: 0.0035 mM.

$$rUR1 \text{ and } rGUR1: v = \frac{V_{UR} \times PIIUMP}{(1 + (K_{GLN}/GLN)) (K_{PIIUMPj} + PIIUMP + PIIUMP2 + PIIUMP3)}$$

V.UR: 5.5e-4 mM/s, K_{GLN} : 0.07 mM (GlnB) and 0.04 mM (GlnK), $K_{PIIUMPj}$: 0.0023 mM.

$$rUR2 \text{ and } rGUR2: v = \frac{V_{UR} \times PIIUMP2}{(1 + (K_{GLN}/GLN)) (K_{PIIUMPj} + PIIUMP + PIIUMP2 + PIIUMP3)}$$

V.UR: 5.5e-5 mM/s, K_{GLN} : 0.07 mM (GlnB) and 0.04 mM (GlnK), $K_{PIIUMPj}$: 0.0023 mM.

$$rUR3 \text{ and } rGUR3: v = \frac{V_{UR} \times PIIUMP3}{(1 + (K_{GLN}/GLN)) (K_{PIIUMPj} + PIIUMP + PIIUMP2 + PIIUMP3)}$$

V.UR: 5.5e-5 mM/s, K_{GLN} : 0.07 mM (GlnB) and 0.04 mM (GlnK), $K_{PIIUMPj}$: 0.0023 mM.

$$rAD: v = \frac{V_{AD} (B_2 + (B_3 \times PIIKG/A \times K_{PIIKG}))}{1 + (K_{GLN}/GLN) + (PIIKG \times K_{GLN}/K_{PIIKG} \times GLN) + (PIIKG/A \times K_{PIIKG})} \frac{GS}{K_{GS} + GS}$$

V.AD: 0.008 mM/s, K_{GLN} : 1 mM, K_{PIIKG} : 1e-5 mM, K_{GS} : 0.0017 mM.

$$rdeAD: v = \frac{V_{DEAD} ((B_2 \times GLN/K_{GLN}) + (B_3 \times PIIUMP/K_{PIIUMP}) + (B_4 \times PIIKG \times GLN/A_1 \times K_{PIIKG} \times K_{GLN})) (GSAMP/K_{GSAMP} + GSAMP)}{1 + (PIIKG/K_{PIIKG}) + (GLN/K_{GLN}) + (PIIUMP/K_{PIIUMP}) + (PIIKG \times GLN/A_1 \times K_{PIIKG} \times K_{GLN}) + (PIIKG \times PIIUMP/K_{A_2} \times K_{PIIKG} \times K_{PIIUMP}) + (GLN \times PIIUMP/K_{A_3} \times K_{GLN} \times K_{PIIUMP}) + (PIIKG \times GLN \times PIIUMP/K_{A_4} \times K_{PIIKG} \times K_{GLN} \times K_{PIIUMP})}$$

V.DEAD: 0.05 mM/s, K_{GLN} : 0.044 mM, K_{PIIUMP} : 1.8e-5 mM, K_{PIIKG} : 4e-6 mM, K_{GSAMP} : 2e-4 mM, A_1 : 0.023, A_2 : 0.88, A_3 : 8.49, A_4 : 0.88, B_2 : 2.77, B_3 : 3.23, B_4 : 0.0049.

$$PIIKG = \frac{3PII \times AKG}{K_1 + 3AKG + 3(AKG^2/K_2) + (AKG^3/K_2 \times K_3)}; K_1: 0.005 \text{ mM}, K_2: 0.15 \text{ mM}, K_3: 0.15 \text{ mM}.$$

$$PIIUMPKG = \frac{PIIUMP3 \times AKG^3}{K_1 \times K_2 \times K_3 + 3AKG \times K_2 \times K_3 + 3AKG^2 \times K_3 + AKG^3}; K_1: 0.025 \text{ mM}, K_2: 0.15 \text{ mM}, K_3: 0.15 \text{ mM}.$$

References

- Bostick, D.L., Brooks 3rd., C.L., 2007. Deprotonation by dehydration: the origin of ammonium sensing in the AmtB channel. *PLoS Comput Biol.* 3, e22.
- Bruggeman, F.J., Boogerd, F.C., Westerhoff, H.V., 2005. The multifarious short-term regulation of ammonium assimilation of *Escherichia coli*: dissection using an in silico replica. *FEBS J.* 272, 1965–1985.
- Coutts, G., Thomas, G., Blakey, D., Merrick, M., 2002. Membrane sequestration of the signal transduction protein GlnK by the ammonium transporter AmtB. *EMBO J.* 21, 536–545.

- Durand, A., Merrick, M., 2006. In vitro analysis of the *Escherichia coli* AmtB-GlnK complex reveals a stoichiometric interaction and sensitivity to ATP and 2-oxoglutarate. *J. Biol. Chem.* 281, 29558–29567.
- Fong, R.N., Kim, K.S., Yoshihara, C., Inwood, W.B., Kustu, S., 2007. The W148L substitution in the *Escherichia coli* ammonium channel AmtB increases flux and indicates that the substrate is an ion. *Proc. Natl. Acad. Sci. U.S.A.* 104, 18706–18711.
- Gruswitz, F., O'Connell 3rd, J., Stroud, R.M., 2007. Inhibitory complex of the transmembrane ammonia channel, AmtB, and the cytosolic regulatory protein, GlnK, at 1.96 Å. *Proc. Natl. Acad. Sci. U.S.A.* 104, 42–47.
- Heeswijk, W.v., 1998. The glutamine synthetase cascade: a search for its control and regulation. PhD Thesis. Free University of Amsterdam, the Netherlands.

- Hoops, S., Sahle, S., Gauges, R., Lee, C., Pahle, J., Simus, N., Singhal, M., Xu, L., Mendes, P., Kummer, U., 2006. COPASI—a COmplex PATHway Simulator. *Bioinformatics* 22, 3067–3074.
- Ikeda, T.P., Shauger, A.E., Kustu, S., 1996. Salmonella typhimurium apparently perceives external nitrogen limitation as internal glutamine limitation. *J. Mol. Biol.* 259, 589–607.
- Ishihama, Y., Schmidt, T., Rappsilber, J., Mann, M., Hartl, F.U., Kerner, M.J., Frishman, D., 2008. Protein abundance profiling of the *Escherichia coli* cytosol. *BMC Genomics* 9, 102.
- Javelle, A., Lupo, D., Li, X.D., Merrick, M., Chami, M., Ripoche, P., Winkler, F.K., 2007. Structural and mechanistic aspects of Amt/Rh proteins. *J. Struct. Biol.* 158, 472–481.
- Javelle, A., Lupo, D., Ripoche, P., Fulford, T., Merrick, M., Winkler, F.K., 2008. Substrate binding, deprotonation, and selectivity at the periplasmic entrance of the *Escherichia coli* ammonia channel AmtB. *Proc. Natl. Acad. Sci. U.S.A.* 105, 5040–5045.
- Javelle, A., Merrick, M., 2005. Complex formation between AmtB and GlnK: an ancestral role in prokaryotic nitrogen control. *Biochem. Soc. Trans.* 33, 170–172.
- Javelle, A., Severi, E., Thornton, J., Merrick, M., 2004. Ammonium sensing in *Escherichia coli*. Role of the ammonium transporter AmtB and AmtB-GlnK complex formation. *J. Biol. Chem.* 279, 8530–8538.
- Javelle, A., Thomas, G., Marini, A.M., Kramer, R., Merrick, M., 2005. In vivo functional characterization of the *Escherichia coli* ammonium channel AmtB: evidence for metabolic coupling of AmtB to glutamine synthetase. *Biochem. J.* 390, 215–222.
- Khademi, S., O'Connell 3rd, J., Remis, J., Robles-Colmenares, Y., Miercke, L.J., Stroud, R.M., 2004. Mechanism of ammonia transport by Amt/MEP/Rh: structure of AmtB at 1.35 Å. *Science* 305, 1587–1594.
- Kleiner, D., 1985. Energy expenditure for cyclic retention of NH₃/NH₄⁺ during N₂ fixation by *Klebsiella pneumoniae*. *FEBS Lett.* 187, 237–239.
- Lin, Y., Cao, Z., Mo, Y., 2006. Molecular dynamics simulations on the *Escherichia coli* ammonia channel protein AmtB: mechanism of ammonia/ammonium transport. *J. Am. Chem. Soc.* 128, 10876–10884.
- Luzhkov, V.B., Almlof, M., Nervall, M., Aqvist, J., 2006. Computational study of the binding affinity and selectivity of the bacterial ammonium transporter AmtB. *Biochemistry* 45, 10807–10814.
- Mathai, J.C., Sprott, G.D., Zeidel, M.L., 2001. Molecular mechanisms of water and solute transport across archaeobacterial lipid membranes. *J. Biol. Chem.* 276, 27266–27271.
- Nielsen, J., Villadsen, J., Lidén, G., 2003. *Bioreaction Engineering Principles*. Springer.
- Reitzer, L., 2003. Nitrogen assimilation and global regulation in *Escherichia coli*. *Annu. Rev. Microbiol.* 57, 155–176.
- van Heeswijk, W.C., Molenaar, D., Hoving, S., Westerhoff, H.V., 2009. The pivotal regulator GlnB of *Escherichia coli* is engaged in subtle and context-dependent control. *FEBS J.* 276, 3324–3340.
- Winkler, F.K., 2006. Amt/MEP/Rh proteins conduct ammonia. *Pflugers Arch.* 451, 701–707.
- Yang, H., Xu, Y., Zhu, W., Chen, K., Jiang, H., 2007. Detailed mechanism for AmtB conducting NH₄⁺/NH₃: molecular dynamics simulations. *Biophys. J.* 92, 877–885.
- Zheng, L., Kostrewa, D., Berneche, S., Winkler, F.K., Li, X.D., 2004. The mechanism of ammonia transport based on the crystal structure of AmtB of *Escherichia coli*. *Proc. Natl. Acad. Sci. U.S.A.* 101, 17090–17095.